Transition of chromium oxyhydroxide nanomaterials to chromium oxide – a Hot Stage Raman spectroscopic study

Jing (Jeanne) Yang, Wayde N. Martens and Ray L. Frost•

Chemistry Discipline, Faculty of Science and Technology, Queensland University of Technology, GPO Box 2434, Brisbane Queensland 4001, Australia

ABSTRACT

The transition of disc-like chromium hydroxide nanomaterials to chromium oxide nanomaterials has been studied by hot stage Raman spectroscopy. The structure and morphology of α-CrO(OH) synthesised using hydrothermal treatment was confirmed by X-ray diffraction and transmission electron microscopy. The Raman spectrum of α-CrO(OH) is characterised by two intense bands at 823 and 630 cm^{-1} attributed to ν_1 Cr^{III}-O symmetric stretching mode, bands at 1179 cm^{-1} attributed to Cr^{III}-OH δ deformation modes. No bands are observed above 3000 cm^{-1}. The absence of characteristic OH vibrational bands may be due to short hydrogen bonds in the α-CrO(OH) structure. Upon thermal treatment of α-CrO(OH), new Raman bands are observed at 599, 542, 513, 396, 344 and 304 cm^{-1}, which are attributed to Cr_2O_3. This hot-stage Raman study shows that the transition of α-CrO(OH) to Cr_2O_3 occurs before 350 °C.

KEYWORDS: Raman spectroscopy, hot stage Raman, chromium oxyhydroxide, chromium oxide, nanomaterials

• Author to whom correspondence should be addressed (r.frost@qut.edu.au)

INTRODUCTION

In recent years, nano-scaled inorganic materials, particularly transition metal based materials, have received more and more attention in industry, in heterogenous catalysis, as support materials as well as active components. Because of their high surface area, chemical and thermally stable properties and mesoporous properties, metal oxides have been extensively used as carriers and support for a variety of industrial catalysts at high temperature as well as low temperature. Novel nanomaterials may be based upon boehmite,[1, 2] titania,[3] gallium oxyhydroxide [4, 5] and designed clay minerals.[6, 7] Special attention has been focused on the formation and properties of chromium oxyhydroxides (CrO(OH)) and chromia (Cr_2O_3), which are important in specific applied applications such as in high-temperature resistant materials,[8, 9] liquid crystal displays,[10, 11] catalysts,[12, 13] and so on. It is well known that intrinsic properties of inorganic materials are mainly determined by their composition, structure, crystallinity, size and morphology; great efforts have been devoted to the investigation of different chromium oxide materials synthesis.[14-16] 3-5 nm CrO(OH) nanocrystals have been prepared by critical CO_2 extraction of the urea-assisted wet chromia gel mixture,[17] and smaller CrO(OH) crystals with size of 1-2 nm were obtained in Chromia aerogel as well.[13] To our best knowledge, 10 nm CrO(OH) synthesised in this work is the biggest hydrothermally synthetic CrO(OH) nanocrystal size so far.

As the development of all kinds of nanomaterials, technologies meet big challenge to achieve perfect control on nanoscal-related properties. Modern Raman instruments offer great advantages to assess some properties that are characteristic of the nanoscale. Many minerals both natural and synthetic lend themselves to analysis by Raman spectroscopy.[18-21] The combination of Raman spectroscopy and a hot stage [22-24] has been proved to be a powerful tool for studying the chemical reactions during dehydration and dehydroxylation. The advantage of this technique is that the changes in molecular structure can be followed in situ and at the elevated temperatures. The purpose of this study is to elucidate the use of hot stage Raman spectroscopy to assess the thermal stability of chromium oxyhydroxide nanomaterials, and to determine the changes in the

59 molecular structure of the nano-scaled materials as the chromium oxyhydroxide is
60 thermally treated. In the present work, the authors report the hot stage Raman spectra of
61 synthetic chromium oxyhydroxide nanomaterial, and the transition of CrO(OH) to Cr_2O_3
62 relating the spectra to the structure of the synthesised materials.
63
64 **EXPERIMENTAL**
65
66 ***Synthesis of CrO(OH) nanomaterial***
67 15 g of $Cr(NO_3)_3 \bullet 9H_2O$ was dissolved in 75 mL ultrapure water, and 28 % ammonia was
68 diluted into 10 % solution. At room temperature, the ammonia solution (10 %) was added
69 at a rate of 1 mL/min into the chromium ion solution with vigorous stirring. Ammonia
70 solution addition ceased when the pH of the reaction mixture reached 5.0. The reaction
71 mixture was kept stirring constantly in the air at room temperature for 0.5 h. The obtained
72 gel-like mixture was centrifuged and washed at 13000 rpm for 10 mins, 3 times. The
73 washed wet gel was transferred into a glass beaker (25 mL). The beaker was placed into a
74 Teflon vessel; 2 mL pure water was poured into the button of the Teflon. The Teflon
75 vessel was then sealed and placed in a 170 ºC oven to process a 12 h steam-assisted
76 hydrothermal treatment. Ultra pure water was added to the resultant product and then
77 collected by centrifugation (at 13000 rpm for 10 mins). The washing process was
78 repeated for 3 times. Sample was dried at 65 ºC overnight.
79
80 ***X-ray diffraction***
81 X-ray diffraction (XRD) analyses were performed on a PANalytical X'Pert PRO X-ray
82 diffractometer (radius: 240.0 mm). Incident X-ray radiation was produced from a line
83 focused PW3373/10 Cu X-ray tube, operating at 40 kV and 40 mA, with Cu Kα
84 radiation of 1.540596 Å. The incident beam passed through a 0.04 rad soller slit, a 1/2 °
85 divergence slit, a 15 mm fixed mask, and a 1 ° fixed antiscatter slit.
86
87 ***Transmission electron microscopy***

A Philips CM20 transmission electron microscope (TEM) at 160 kV was used to investigate the morphology of the as-prepared sample. The sample was ultrasonically dispersed in absolute ethanol solution, and then dropped on copper grid, which dried in the air.

Raman microprobe spectroscopy

The crystals of CrO(OH) were placed and oriented on the stage of an Olympus BHSM microscope, equipped with 10x and 50x objectives and part of a Renishaw 1000 Raman microscope system, which also includes a monochromator, a filter system and a Charge Coupled Device (CCD). Raman spectra were excited by a 633 nm laser at a resolution of 2 cm^{-1} in the range between 100 and 4000 cm^{-1}. Repeated acquisition using the highest magnification was accumulated to improve the signal-to-noise ratio. Spectra were calibrated using the 520.5 cm^{-1} line of a silicon wafer. Details of the technique have been published by the authors. [22-27] Spectra at elevated temperatures were obtained using a Linkam thermal stage (Scientific Instruments Ltd., Waterford Surrey, England). Spectra were taken from room temperature (25 ºC) up to a temperature of 550 ºC in a flowing nitrogen atmosphere. Spectral Manipulation such as baseline adjustment, smoothing and normalisation was performed using GRAMS® software package (Galactic Industries Corporation Salem, NH, USA).

Band component analysis was undertaken using the Jandel 'Peakfit' software package, which enabled the type of fitting function to be selected and allows specific parameters to be fixed or varied accordingly. Band fitting was sone using a Lorentz-Gauss cross-product function with the minimum number of component bands used for the fitting process. The Lorentz-Gauss ratio was maintained at values greater than 0.7 and fitting was undertaken until reproducible results were obtained with squared correlations of r^2 greater than 0.996.

RESULTS AND DISCUSSION

Phase Structure and morphology of the synthetic α-CrO(OH) nanomaterial

X-ray diffraction (XRD) was used to determine the phase structure of the hydrothermally synthesised material. It is reported that chromium oxyhydroxides can crystallised in three polymorphs, α, β and γ.[28] The α-CrO(OH) phase has a layer crystal structure with trigonal symmetry (space group R-3*m* or R3*m*).[29] β-CrO(OH) has a different structure from α-CrO(OH) and consist of a distorted rutile-type structure with orthorhombic symmetry (space group P*nnm* or $P2_1nm$).[30] γ-CrO(OH) was reported to be X-ray amorphous[28] and assumed to have the same structure as boehmite, γ -AlO(OH).[31, 32] α-CrO(OH) is found as grimaldiite a naturally occurring mineral, while β-CrO(OH) is found as guyanite, another mineral phase.[33]

Fig. 1 presents the typical XRD pattern of the resultant material. All diffraction peaks in this pattern are well indexed and in good agreement with the standard JCPDS card No. 01-085-1374 (Grimaldiite). No impurity peaks are observed, indicating that the resultant material was a single crystalline phase, α-CrO(OH). The rhombohedral unit cell of α-CrO(OH) (space group R3*m*) is shown in Fig. 2a, presenting a three-layered structure. The parameters for this unit cell are: a = b = 2.979 Å, c = 13.70 Å.[34] As reported by Christensen[34] and Fujihara[35], in the structure of α-CrO(OH) , layers of Cr atoms perpendicular to the trigonal axis are sandwiched between two parallel sheets of oxygen atoms, which are joined by short hydrogen bonds aligned along the trigonal axis (Fig. 2a). It is easily observed in the structure (Fig. 2b) that 6 oxygen atoms are octahedrally coordinated about each chromium atom, and each oxygen atom was coordinated by three chromium atoms. Hydrogen atoms are assumed to be involved in a disordered structure.

Morphology of the synthetic α-CrO(OH) material was examined using transmission electron microscopy (TEM), as shown in Fig. 3. Because of the high surface energy of

nano-particles, nanocrystals in the TEM image are aggregated. However we can still observe that the synthetic α-CrO(OH) crystals have an overall shape of discs with average size of 10 nm in diameter. The size of synthetic α-CrO(OH) nanocrystals observed from TEM is in accordance with the result estimated by Scherrer equation from the XRD data, which was 11 nm.

Hot-stage Raman spectroscopy

Raman spectra of α-CrO(OH)

In order to study the changes in the spectra of α-CrO(OH) as the nanomaterial is thermally treated, it is necessary to describe the spectra collected at low temperature. According to the previous thermogravimetric study published by the authors, the dehydration of α-CrO(OH) was observed from 120 °C. Therefore, this study reported the spectra before and after 120 °C and will discussion the structure change of the material during the thermal decomposition process. Fig. 4 depicts the Raman spectra at 25 and 100 °C of α-CrO(OH) nanomaterial in the region of 200 to 1800 cm^{-1}. The spectra are characterised by two intense bands at 823 and 630 cm^{-1}. As discussed above, α-CrO(OH) adopts the sheet structure built from [$Cr^{III}O_6$] octahedra. Bands at 823 and 630 cm^{-1} are attributed to the ν_1 Cr^{III}-O symmetric stretching vibration. An additional band is found at 558 cm^{-1}. This band is attributed to the ν_3 Cr^{III}-O anti-symmetric stretching vibration. A low intensity band is observed at 452 cm^{-1}, which is assigned to the O-Cr^{III}-O bending modes. This is in good agreement with the reports by Maslar *et al.*[36] Low intensity Raman bands are found at the 985-889 cm^{-1} region, however this wavenumber range is too high to due to Cr^{III}-O vibrational modes, and is assumed to be the Cr^{VI}-O stretching modes or mixed Cr^{III}/Cr^{VI} –O vibrational modes as reported by Maslar *et al.*.[37, 38] Maslar published Raman studies on chromium coupons, and α-CrO(OH) was identified as a corrosion product. It is possible to detected trace of Cr (VI) in the resultant sample due to the hydrothermal treatment, where little portion of Cr (III) material can be oxidised to Cr (IV) compounds in the high temperature and high pressure conditions. Moreover, Raman spectroscopy once again shows its advantage as a powerful tool to examine the phases

trace in the samples, when the content of materials is too little to be detected by bulk technique, such as XRD.

In the region of 1000 to 1200 cm^{-1}, the Raman spectra at 25 and 100 °C are composed of broad low intensity bands. These bands are assigned to Cr^{III}-OH δ deformation modes. Raman spectra of some crystalline oxyhydroxides exhibit OH stretching modes in the region above 3000 cm^{-1}. However, no obvious bands are observed in this wavenumber range. This lack of characteristic OH vibrational bands is possible due to the short hydrogen bonds in the α-CrO(OH) structure. This observation is accordant with the reports made by Christensen[28], which revealed no OH absorption was found in an infrared study. An intense band at 1607 cm^{-1} is presented in the Raman spectrum of 25 °C, which shifts to 1593 cm^{-1} in the 100 °C spectrum. These bands are assumed to the bending modes of absorbed water in the α-CrO(OH) layered structure.

Thermal transition from α-CrO(OH) to Cr_2O_3 nanomaterials

The hot stage Raman spectroscopy of the transition of α-CrO(OH) to Cr_2O_3 in the region of 200 to 1800 cm^{-1} over the temperature range ambient to 550 °C is studied in this work. The Raman spectrum at 350 °C shows different features from that at low temperatures (25 and 100 °C) in Fig. 5. Bands at 1607, 1171, 823, 630, 556 and 425 cm^{-1} are not observed anymore. New Raman bands at 602, 544, 518, 389, 348 and 304 cm^{-1} are found, which are attributed to the new phase (Cr_2O_3) formed by the thermal decomposition of chromium oxyhydroxide. It is reported that Cr_2O_3 adopts the corundum (Al_2O_3) structure consisting of vertex-, edge-, and face-sharing [$Cr^{III}O_6$] octahedral.[36] Kemdehoundja *et al.* discussed that there are five vibrational modes for chromia, four E_g modes and one A_{1g} mode.[39] Chen *et al.* reported as well that Cr_2O_3 presented the most intense A_{1g} band at 540 cm^{-1}, with another two lower intensity bands at 291 and 335 cm^{-1}.[40] A sharp band was observed at 1009 cm^{-1} with a shoulder at 997 cm^{-1}. These bands are assumed to due to O-H deformation modes.

Broad bands are observed in the region of 620-830 cm^{-1}, which are assigned to the vibrations of Cr^{VI}-O bridging bonds. It is reported that Cr^{VI} is probably present in brdging

bonds but not in polychromate structures.[36] In such structures, Cr^{VI} is incorporated into the Cr^{III}-O surface network rather than being present as a monochromate or polychromate. There is a small band found at 1363 cm^{-1} at the temperature of 350 °C, which is assigned to be the combination band.

The Raman spectrum at 550 °C is very similar with what that at 350 °C, which indicated the thermal decomposition product from α-CrO(OH) nanomaterial is Cr_2O_3. Bands in 620-830 cm^{-1} region show the loss of intensity at 550 °C. The combination band at 1363 cm^{-1} disappeared at 550 °C. No intensity of OH stretching bands remained at 550 °C, which reveals that α-CrO(OH) had totally transformed to Cr_2O_3. This agrees with the results of thermal gravimetric analysis reported in somewhere else by the authors, which showed no sample mass loss above 550 °C. All the peaks and their assignment are summarised in Table 1.

CONCLUSIONS

Disc-like of α-CrO(OH) nanomaterial was synthesised by using hydrothermal techniques without surfactants at low temperatures. The phase composition was proven by X-ray diffraction and TEM showed a10 nm size of the nanocrystals. The conversion of α-CrO(OH) to Cr_2O_3 nanomaterial was achieved by thermal treatment up to 350 °C. The transition of α-CrO(OH) to Cr_2O_3 was studied by hot stage Raman spectroscopy; upon thermally treating the synthetic α-CrO(OH) nanomaterial at 550 °C.

The structure of synthetic nanomaterials, α-CrO(OH) and Cr_2O_3, are deduced from their Raman spectra. Intense bands at 823 and 630 cm^{-1}, as well as relatively weaker peaks at 558 and 452 cm^{-1} were observed in the Raman spectra of rhombohedral α-CrO(OH). These bands are attributed to O-Cr^{III}-O vibrations. Bands at 1179 cm^{-1} are assigned to Cr^{III}-OH δ deformation modes. Upon thermal treatment of α-CrO(OH) at 350 °C, new Raman bands at 599, 542, 513, 396, 344 and 304 cm^{-1} are found. The Raman spectrum of resultant Cr_2O_3 is characterised by an intense sharp peak at 542 cm^{-1}, which was due to the A_{1g} band.

ACKNOWLEDGMENT

The financial and infra-structure support of the Queensland University of Technology Inorganic Materials Research Program is gratefully acknowledged. The Australian Research Council (ARC) is thanked for funding the instrumentation. One of the authors (JY) is grateful to the Queensland University of Technology Inorganic Materials Research Program for the award of an international doctoral scholarship.

REFERENCES

[1] J. Yang, R. L. Frost, Y. Yuan, *Thermochimica Acta* **2009,** *483,* 29-35.

[2] J. Yang, Y. Zhao, R. L. Frost, *Appl. Surf. Sci.* **2009,** *255,* 7925-7936.

[3] X. Yang, D. Yang, H. Zhu, J. Liu, W. N. Martins, R. Frost, L. Daniel, Y. Shen, *J. Phys. Chem. C* **2009,** *113,* 8243-8248.

[4] Y. Zhao, R. L. Frost, *Journal of Raman Spectroscopy* **2008,** *39,* 1494-1501.

[5] Y. Zhao, R. L. Frost, J. Yang, W. N. Martens, *Journal of Physical Chemistry C* **2008,** *112,* 3568-3579.

[6] L. M. Daniel, R. L. Frost, H. Y. Zhu, *Journal of Colloid and Interface Science* **2008,** *321,* 302-309.

[7] L. M. Daniel, R. L. Frost, H. Y. Zhu, *Journal of Colloid and Interface Science* **2008,** *322,* 190-195.

[8] M. Nofz, R. Sojref, M. Feigl, M. Dressler, I. Doerfel, *Keram. Z.* **2009,** *61,* 272,274-277.

[9] X. Yang, X. Peng, C. Xu, F. Wang, *J. Electrochem. Soc.* **2009,** *156,* C167-C175.

[10] J. Fujikawa, M. Hata, K. Kokaji, Direct-current reactive sputtering for metal compound thin film without unreacted metal particles. (Nippon Electric Glass Co., Ltd., Japan). JP, 1998, p. 5.

[11] K. Shigeta, K. Goto, Electron emitters having layers with controlled perpendicular and horizontal resistivity. (Toray Industries, Inc., Japan). JP, 2009, p. 10.

[12] H. Rotter, M. V. Landau, M. Carrera, D. Goldfarb, M. Herskowitz, *Appl. Catal., B* **2004,** *47,* 111-126.

[13] H. Rotter, M. V. Landau, M. Herskowitz, *Environ. Sci. Technol.* **2005,** *39,* 6845-6850.

[14] M. Abecassis-Wolfovich, H. Rotter, M. V. Landau, E. Korin, A. I. Erenburg, D. Mogilyansky, E. Garshtein, *Stud. Surf. Sci. Catal.* **2003,** *146,* 247-250.

[15] Y.-L. Bai, H.-B. Xu, Y. Zhang, Z.-H. Li, *J. Phys. Chem. Solids* **2006,** *67,* 2589-2595.

[16] M. V. Landau, G. E. Shter, L. Titelman, V. Gelman, H. Rotter, G. S. Grader, M. Herskowitz, *Ind. Eng. Chem. Res.* **2006,** *45,* 7462-7469.

[17] M. Abecassis-Wolfovich, H. Rotter, M. V. Landau, E. Korin, A. I. Erenburg, D. Mogilyansky, E. Gartstein, *J. Non-Cryst. Solids* **2003,** *318,* 95-111.

[18] R. L. Frost, J. T. Kloprogge, *Appl. Spectrosc.* **1999,** *53,* 1610-1616.

[19] Y. Zhao, J. Yang, R. L. Frost, *J. Raman Spectrosc.* **2008,** *39,* 1327-1331.
[20] Y. Y. Zhao, R. L. Frost, *J. Raman Spectrosc.* **2008,** *39,* 1494-1501.
[21] J. Yang, H. Liu, W. N. Martens, R. L. Frost, *J. Phys. Chem. C* **2010,** *114,* 111-119.
[22] R. L. Frost, S. Bahfenne, *J. Raman Spectrosc.* **2010,** *41,* 207-211.
[23] R. L. Frost, S. Bahfenne, *J. Raman Spectrosc.* **2010,** *41,* 325-328.
[24] R. L. Frost, K. H. Bakon, S. J. Palmer, *J. Raman Spectrosc.* **2010,** *41,* 78-83.
[25] R. L. Frost, J. Cejka, J. Sejkora, J. Plasil, S. Bahfenne, S. J. Palmer, *J. Raman Spectrosc.* **2010,** *41,* 571-575.
[26] R. L. Frost, J. Cejka, J. Sejkora, J. Plasil, S. Bahfenne, S. J. Palmer, *J. Raman Spectrosc.* **2010,** *41,* 566-570.
[27] R. L. Frost, J. Sejkora, E. C. Keeffe, J. Plasil, J. Cejka, S. Bahfenne, *J. Raman Spectrosc.* **2010,** *41,* 202-206.
[28] A. N. Christensen, *Acta Chem. Scand., Ser. A* **1976,** *A30,* 133-136.
[29] W. C. Hamilton, J. A. Ibers, *Acta Crystallographica* **1963,** *16,* 1209-1212.
[30] A. N. Christensen, P. Hansen, M. S. Lehmann, *J. Solid State Chem.* **1976,** *19,* 299-304.
[31] J. Yang, R. L. Frost, *Res. Lett. Inorg. Chem.* **2008,** No pp given.
[32] C. Milton, D. E. Appleman, M. H. Appleman, E. C. T. Chao, F. Cuttitta, J. I. Dinnin, E. J. Dwornik, B. L. Ingram, H. J. Rose, Jr., *U. S., Geol. Surv., Prof. Pap.* **1976,** *887,* 29 pp.
[33] A. K. Shpachenko, N. V. Sorokhtina, N. V. Chukanov, A. N. Gorshkov, A. V. Sivtsov, *Geochem. Int.* **2006,** *44,* 681-689.
[34] A. N. Christensen, P. Hansen, M. S. Lehmann, *J. Solid State Chem.* **1977,** *21,* 325-329.
[35] T. Fujihara, M. Ichikawa, T. Gustafsson, I. Olovsson, T. Tsuchida, *Ferroelectrics* **2001,** *259,* 133-138.
[36] J. E. Maslar, W. S. Hurst, W. J. Bowers, J. H. Hendricks, M. I. Aquino, I. Levin, *Appl. Surf. Sci.* **2001,** *180,* 102-118.
[37] J. E. Maslar, W. S. Hurst, T. A. Vanderah, I. Levin, *J. Raman Spectrosc.* **2001,** *32,* 201-206.
[38] J. E. Maslar, W. S. Hurst, W. J. Bowers, J. H. Hendricks, *J. Nucl. Mater.* **2001,** *298,* 239-247.
[39] M. Kemdehoundja, J. L. Grosseau-Poussard, J. F. Dinhut, *Jounal of Applied Physics* **2007,** *102,* 093513.

[40] Y. Chen, K. Ding, L. Yang, B. Xie, F. Song, J. Wan, G. Wang, M. Han, *Appl. Phys. Lett.* **2008,** *92,* 173112/173111-173112/173113.

Table 1

α-CrO(OH) nanomaterial			Cr_2O_3 nanomaterial		
25 °C	**100** °C	**Assignment**	**350** °C	**550** °C	**Assignment**
1634					
1593	**1607**	**Water H-O-H bending**			
1537	**1537**				
1504	**1387**	**Combinations & overtones**			
			1363		**Combinations & overtones**
1179,1153	**1171, 1129**	**O-H deformation**			
			1009, 997	**1007, 997**	**O-H deformation**
981	**985, 938**	**Cr^{VI}-O**			
889	**889**				
			817		
			771	**770**	**Cr^{VI}-O**
			729	**719**	
823	**823**	**ν_1 (O-Cr^{III}-O)**	**683**	**684**	
630	**630**				
558	**556**	**ν_3 (O-Cr^{III}-O)**	**602**	**599**	**Cr_2O_3**
			544, 518	**542, 513**	**Cr_2O_3**
452	**452**	**ν_2 (O-Cr^{III}-O)**		**477**	**Cr^{VI}-O**
			389	**396**	**Cr_2O_3**
			348	**344**	**Cr_2O_3**
			304	**304**	**Cr_2O_3**

ν_1 (O-Cr^{III}-O symmetric stretching);

ν_2 (O-Cr^{III}-O symmetric bending);

ν_3 (O-Cr^{III}-O anti-symmetric stretching)

LIST OF TABLES

LIST OF FIGURES

357

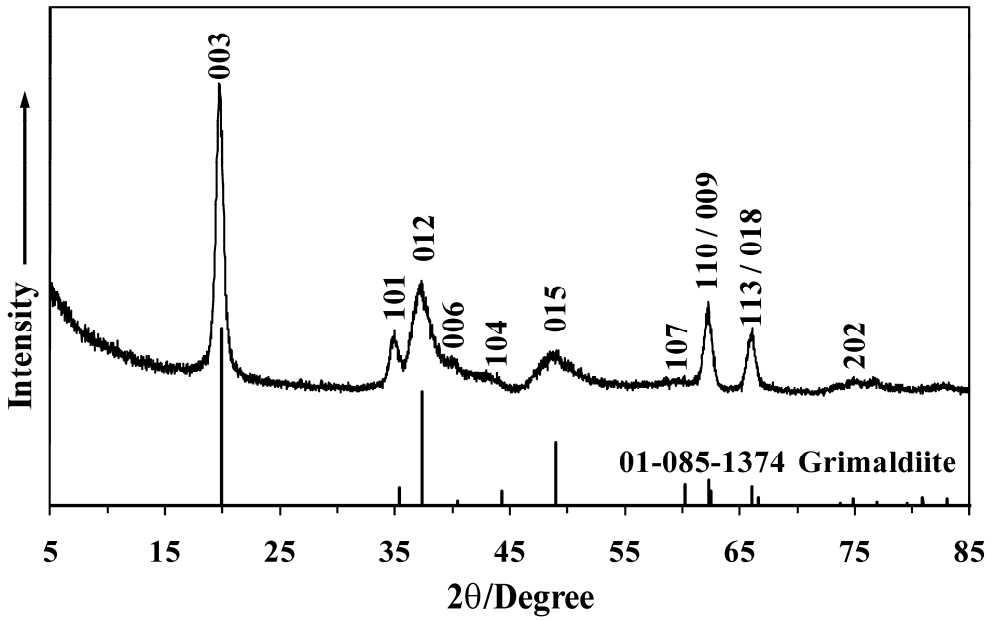

358

359 **Fig. 1**

360

361

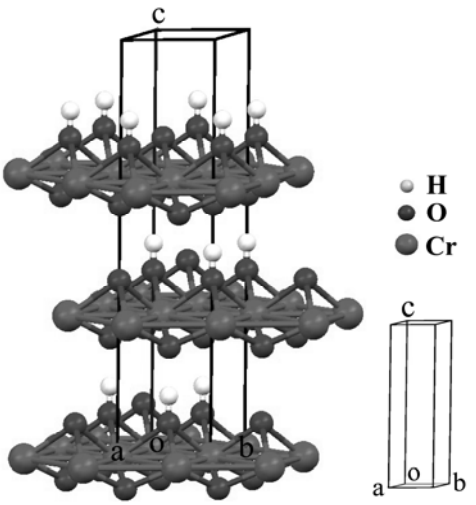

362

363 **Fig. 2a**

364

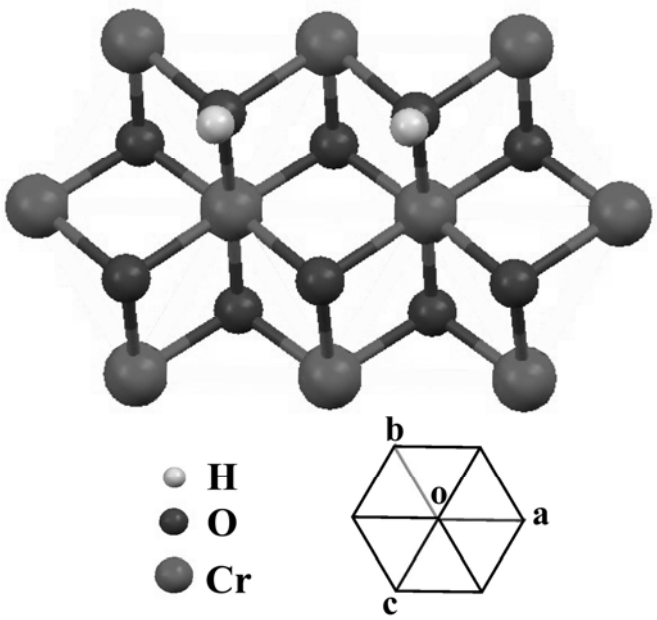

365

366 **Fig. 2b**

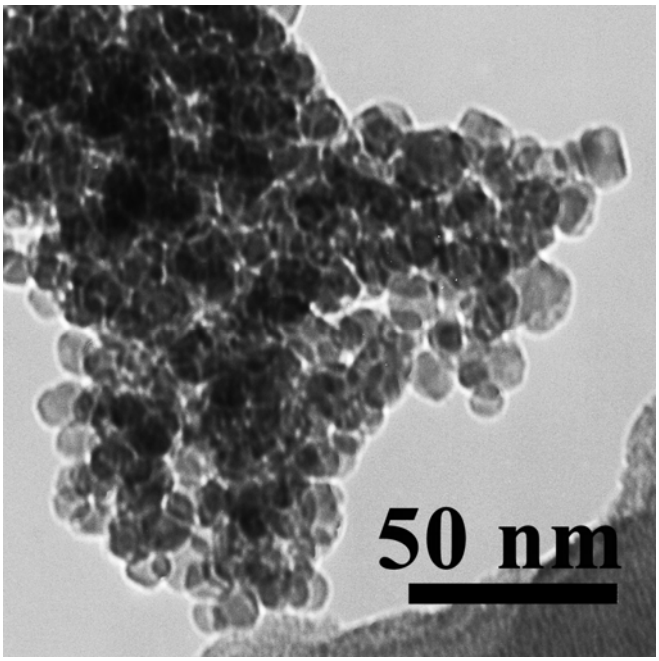

Fig. 3

371

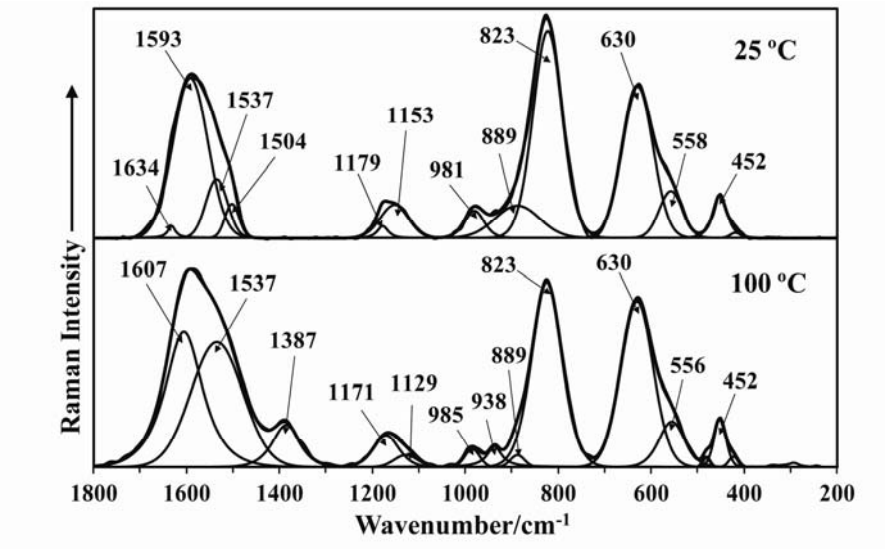

372

373 **Fig. 4**

374

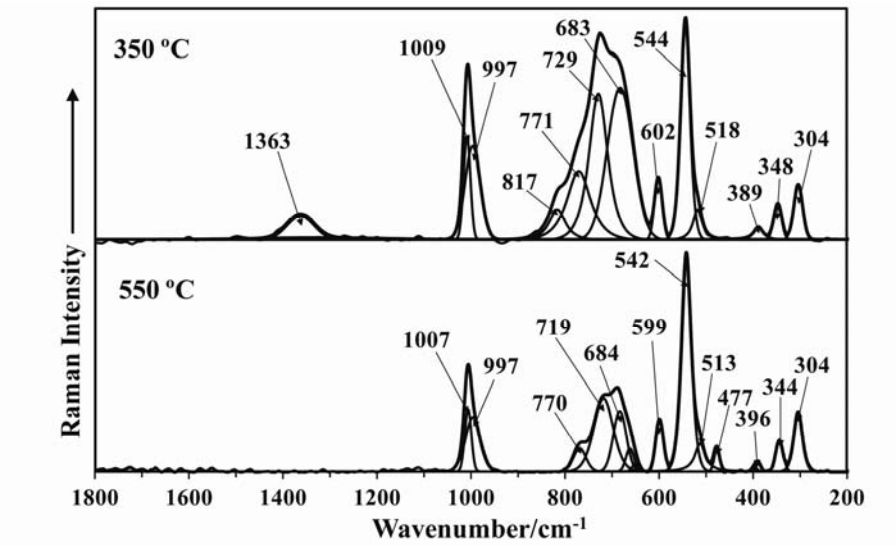
350 °C
1009
997
683
729
544
771
602
518
304
1363
817
348
389
542
550 °C
1007
719
684
599
997
513
304
770
477
344
396
Raman Intensity
1800
1600
1400
1200
1000
800
600
400
200
Wavenumber/cm-1

375

376 **Fig. 5**